Supporting Information for

Artificial Metabolism-Inspired Photoelectrochemical Probing of Biomolecules and Cells

Jing Tang,[a] Yongcheng Wang,[a] Yuhang Wang,[a] Jun Li,[b] Biao Kong,[a] Min Jiang,[c] and Gengfeng Zheng [a,*]

[a] Laboratory of Advanced Materials, Department of Chemistry, Fudan University, Shanghai 200433, P. R. China

[b] School of Pharmacy, Fudan University, Shanghai 201203, China

[c] Institutes of Brain Science and State Key Laboratory of Medical Neurobiology, Fudan University, Shanghai 200032, P. R. China

*Corresponding authors: Gengfeng Zheng

Email addresses: *gfzheng@fudan.edu.cn (G.Z.)*

Supporting Figures

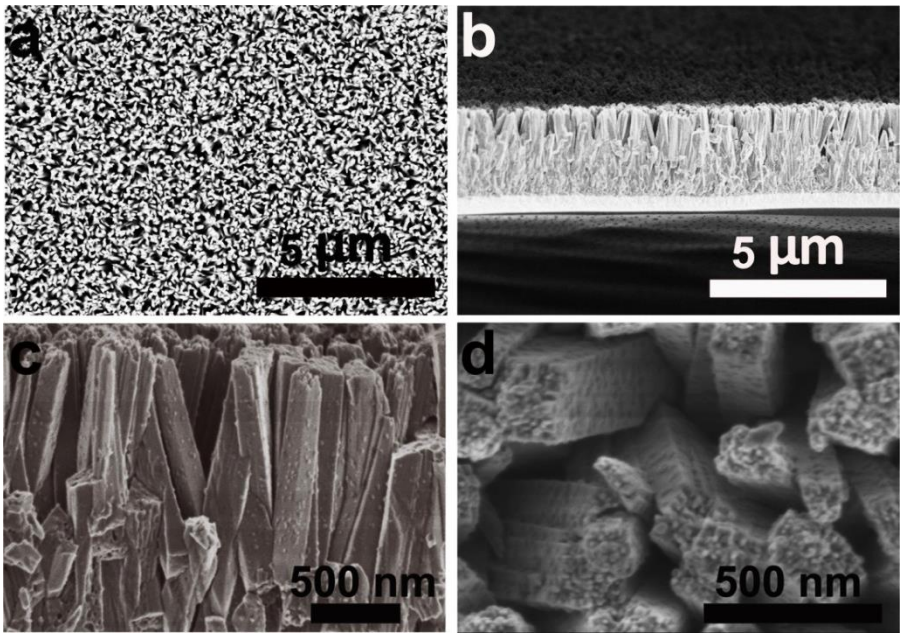

Figure S1. (a, d) Top-view and (b, c) side-view SEM images of TiO_2-Co_3O_4 NW arrays on FTO-coated glass substrates.

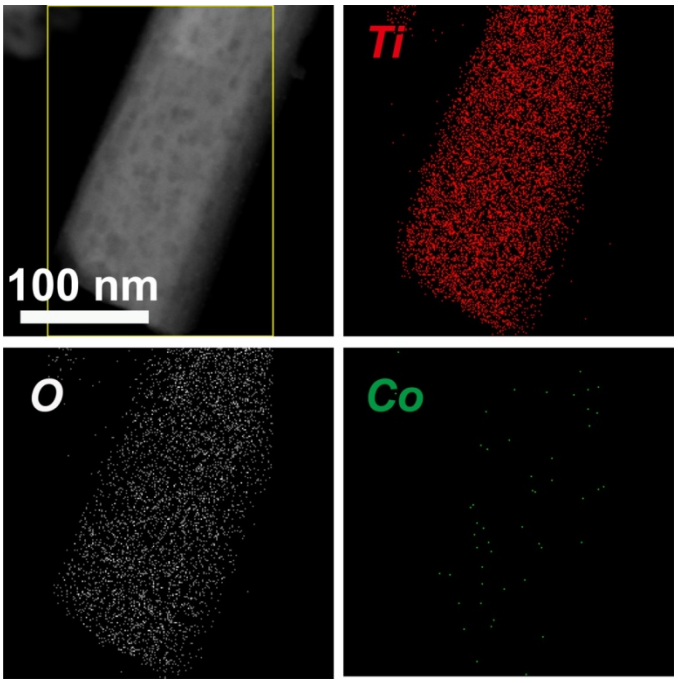

Figure S2. Elemental mapping of a representative TiO_2-Co_3O_4 NW for Ti, O and Co distribution over the NW.

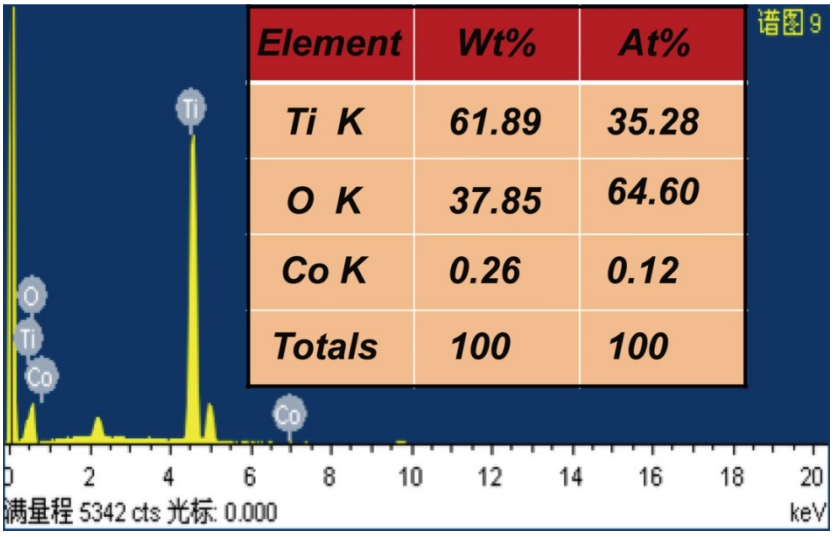

Figure S3. EDX of a representative TiO_2-Co_3O_4 NW.

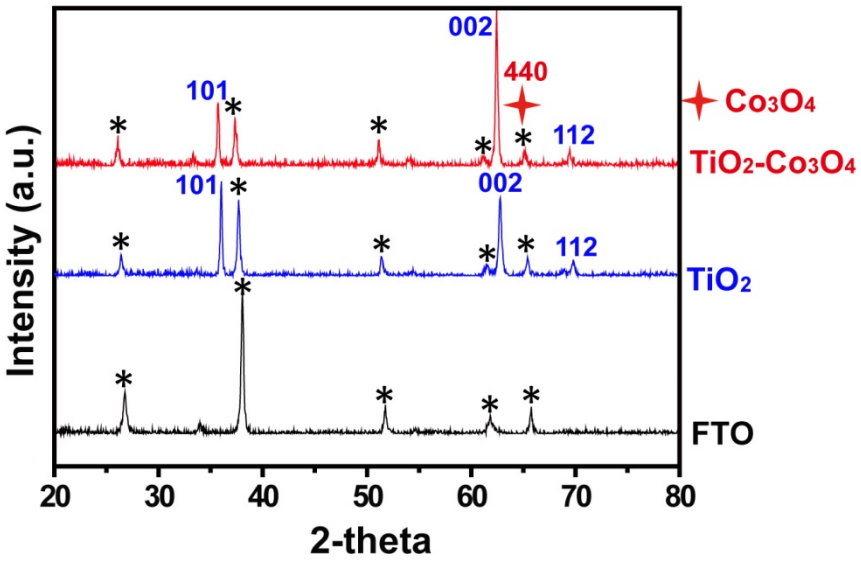

Figure S4. XRD patterns of the pristine TiO_2 NWs (blue curve) and TiO_2-Co_3O_4 NWs (red curve) grown on FTO substrates. XRD pattern of a blank FTO substrate is also displayed for comparison. The peaks of FTO are indicated by asterisks.

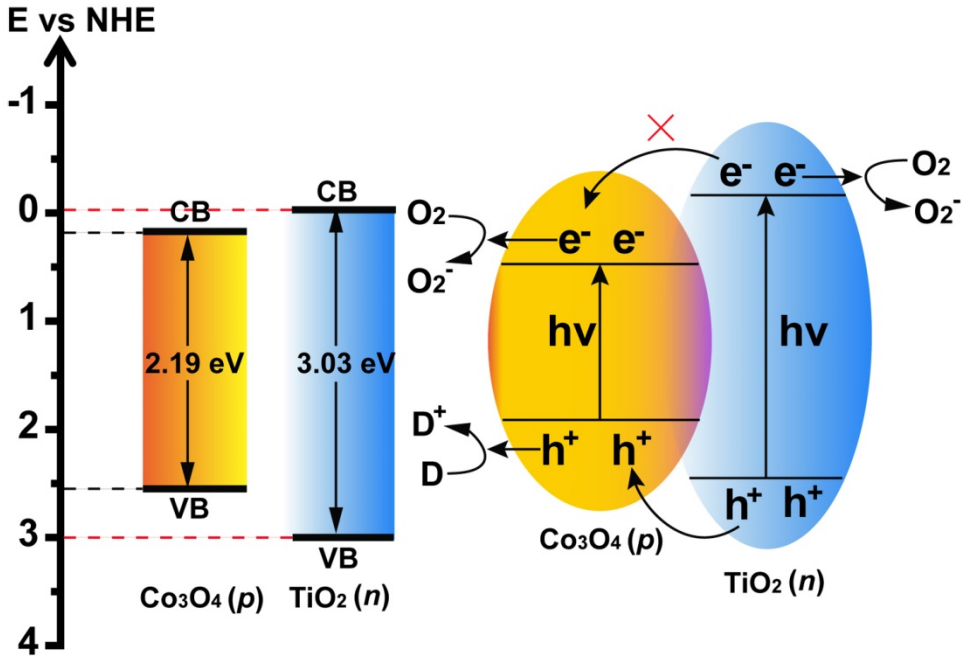

Figure S5. Energy bands of Co_3O_4 and TiO_2, and the electron transfer process of Co_3O_4/TiO_2 interface under a simulated sunlight illumination. All the energy levels are referenced to NHE scale. CB and VB are conduction band and valence band, respectively.

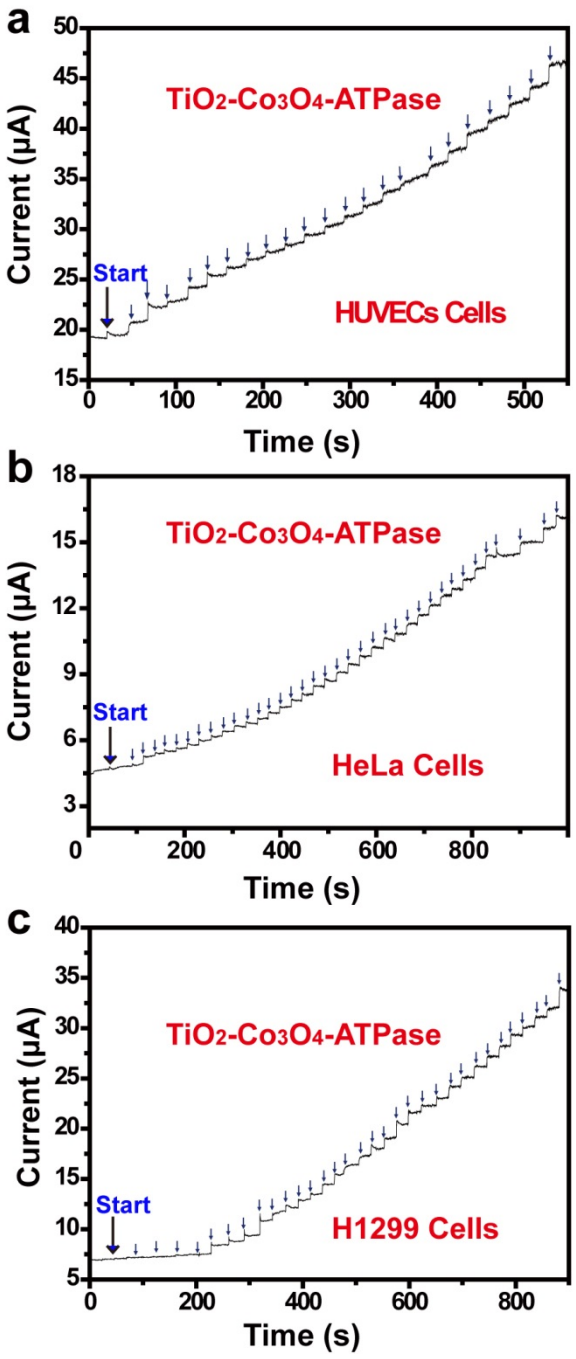

Figure S6. (a, b, c) Photocurrent versus time data of the TiO_2-Co_3O_4-ATPase NWs for cell extracts (1×10^5 cells/mL after 1:100 dilution) from solutions of HUVECs, HeLa and H1299 cells. The sizes of the active sample area were 0.02-0.06 cm^2.

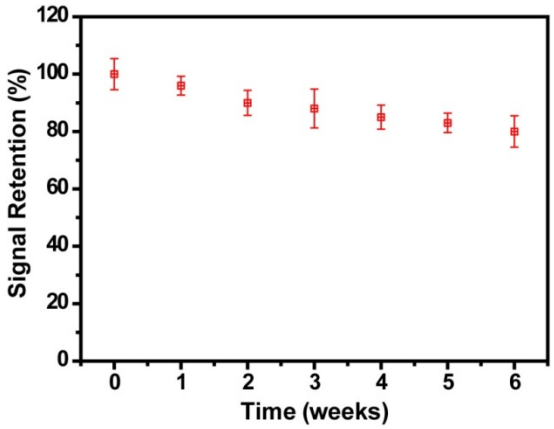

Figure S7. Stability test of a TiO_2-Co_3O_4-ATPase NW biosensor for ATP detection over a month. The sizes of the active sensor surfaces were around 0.02−0.06 cm^2.

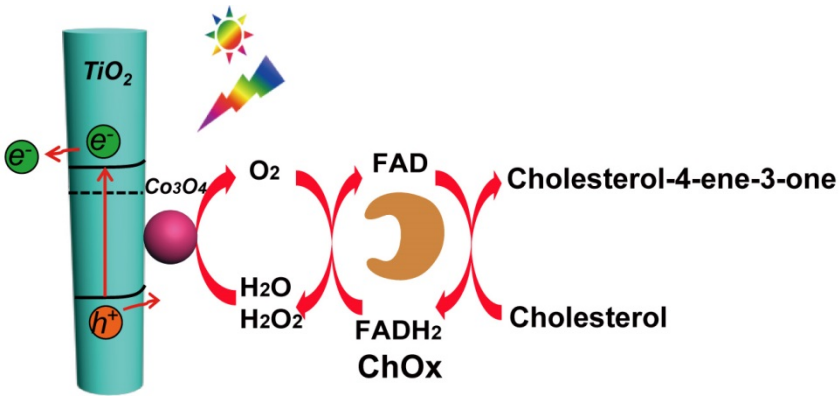

Figure S8. Schematic of the TiO_2-Co_3O_4-ChOx NW-based PEC sensor for cholesterol detection. Under sun light illumination, H_2O or H_2O_2isoxidized by the photogenerated holes over the TiO_2 NW anode to generate O_2, which conducts as an efficient electron acceptor of FAD/$FADH_2$. During this cycle, cholesterol is oxidized to cholesterol-4-ene-3-one. On the cathode (Pt), the photogenerated electrons reduce water to produce H_2. The sensing signal represents the current flowing through the circuit.

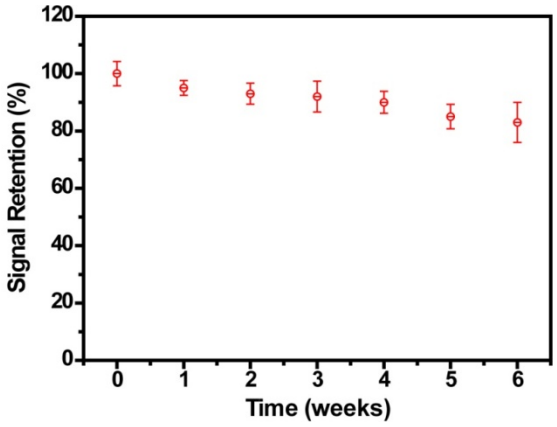

Figure S9. Stability test of a TiO_2-Co_3O_4-ChO_x NW biosensor over a month. The sizes of the active sensor surfaces were around 0.02-0.06 cm^2.

Table S1. Analytical performance of the present integrated TiO_2-Co_3O_4-ATPase NW-based photoelectrochemical detection of ATP, compared to previously reported literatures.

Methods	***Materials***	***Linear Range***	***Detection Limit***	***Reference***
The present method	TiO_2-Co_3O_4-ATPase NWs	0.14nM-10 μM	0.14 nM	The present work
Fluorometry	Ribonucleopeptide	10^{-7}-10^{-3} M	□10^{-7}	S1
	Oligonucleotide	0~2×10^{-6} M	25 nM	S2
	DNA-Ag nanoclusters	0-1000 μM	0.2 μM	S3
Colorimetry	DNAzyme-Aptamer	100 μM	10^{-6} M	S4
Odor-Based Sensor	Tryptophanase	ELISA-like	-	S5
Optical ATP Biosensor	Enzyme	10^{-3} mM to 1.5 mM	1μM	S6
Logic Gates Sensors	Three-Dimensional DNA Nanostructures	0-600 nM	20 nM	S7
FET Sensor	Aptamer	1-1000 μM	1 μM	S8
Chromogenic Sensor	Zn(II)-Cyclam	0~2×10^{-4} M	＜ 0 M	S9
Photoelectrochemical Biosensor	Bio-Barcode Amplification	0-100×10^{-8} M	3.2×10^{-9} M	S10

LOD = limit of detection; LR = linear ranges;

Table S2. Analytical performance of the present integrated TiO_2-Co_3O_4-ChO_x -based photoelectrochemical detection of cholesterol, compared to previously reported literatures.

Methods	***Materials***	***Linear Range***	***Detection Limit***	***Reference***
The present method	TiO_2-Co_3O_4-ChO_x NWs	0.5 nM-50 μM	0.2 nM	The present work
Electrogenerated Chemiluminescence	Hemin-Graphene Nanosheets	0.17 mM to 1.12 mM	0.06 mM	S11
Fluorimetric Biosensors	Alginate-Silica Microspheres	1.25 to 10 mM	less than 1.25 mM	S12
Amperometric Biosensor	Carbon Nanotubes	2.5-10 mM	less than 5 mM	S13
	Chitosan/silica-MWCNT	8.0×10^{-6} mM~0.4 mM	1×10^{-6} mM	S14
	ZnO	1.0 to 700.0 nM	0.37nM	S15
	Pt nanoparticles	Up to 4.0 mM	0.2μM	S16
Electrochemistry	Nickel Oxide-Chitosan Film	10-400 mg/dL	43.4 mg/dL	S17
	Cuprous Oxide/Chitosan	10-450 mg/dL	15.9 mg/dLcm^{-2}	S18
Microfluidics Nanobiochip	nNiO and MWCNTs	0.25-12.93 mM	0.03 mM	S19
	CNT	1.25-10.0 mM	25 mg/dL	S20
	nNiO	1.5-10.3 mM	0.16 mM	S21
Electrochemiluminescence	Luminol			S22

Solution-Gated				
	ZnONanorods	0.001-45 mM	0.05 mM	S23
Feld Effect Transistor				

References:

S1. S. Nakano, M. Fukuda, T. Tamura, R. Sakaguchi, E. Nakata, T. Morii, *J. Am. Chem. Soc.*, 2013, **135**, 3465-3473.

S2. F. Li, Z. Du, L. Yang, B. Tang, *Biosens. Bioelectron.*, 2013, **41**, 907-910.

S3. Z. Zhou, Y. Du, S. Dong, *Biosens. Bioelectron.*, 2011, **28**, 33-37.

S4. F. Liu, J. Zhang, R. Chen, L. Chen, L. Deng, *Chem. Biodivers.*, 2011, **8**, 311-316.

S5. Y. Xu, Z. Zhang, M. M. Ali, J. Sauder, X. Deng, K. Giang, S. D. Aguirre, R. Pelton, Y. Li, C. D. Filipe, *Angew. Chem. Int. Ed.*, 2014, **53**, 2620-2622.

S6. C. Wang, C. Y. C. Huang, W. C. Lin, *Biosens. Bioelectron.*, 2013, **43**, 355-361.

S7. H. Pei, L. Liang, G. Yao, J. Li, Q. Huang, C. Fan, *Angew. Chem. Int. Ed.*, 2012, **124**, 9154-9158.

S8. J. Das, K. B. Cederquist, A. A. Zaragoza, P. E. Lee, E. H. Sargent, S. O. Kelley, *Nat. Chem.*, 2012, **4**, 642-648.

S9. P. Mahato, A. Ghosh, S. K. Mishra, A. Shrivastav, S. Mishra, A. Das, *Inorg. Chem.*, 2011, **50**, 4162-4170.

S10. X. Zhang, Y. Zhao, S. Li, S. Zhang, *Chem. Commun.*, 2010, **46**, 9173-9175.

S11. M. Zhang, R. Yuan, Y. Chai, S. Chen, X. Zhong, H. Zhong, C. Wang, *RSC Adv.*, 2012, **2**, 4639-4641.

S12. J. Liu, Y. Zhang, D. Chen, T. Yang, Z. Chen, S. Pan, N. Gu, *Colloids Surf. A*, 2009, **341**, 33-39.

S13. M. Guo, J. Chen, J. Li, L. Nie, S. Yao, *Electroanalysis*, 2004, **16**, 1992-1998.

S14. X. Tan, M. Li, P. Cai, L. Luo, X. Zou, *Anal. Biochem.*, 2005, **337**, 111-120.

S15. A. Umar, M. M. Rahman, M. Vaseem, Y.-B. Hahn, *Electrochem. Commun.*, 2009, **11**, 118-121.

S16. R. S. Dey, C. R. Raj, *J. Phys. Chem. C*, 2010, **114**, 21427-21433.

S17. J. Singh, P. Kalita, M. K. Singh, B. Malhotra, *Appl. Phys. Lett.*, 2011, **98**, 123702.

S18. J. Singh, M. Srivastava, A. Roychoudhury, D. W. Lee, S. H. Lee, B. Malhotra, *J. Phys. Chem. B*, 2012, **117**, 141-152.

S19. M. A. Ali, S. Srivastava, P. R. Solanki, V. Reddy, V. V. Agrawal, C. Kim, R. John, B. D. Malhotra, *Sci. Rep.*, 2013, **3**.

S20. A. Wisitsoraat, P. Sritongkham, C. Karuwan, D. Phokharatkul, T. Maturos, A. Tuantranont, *Biosens. Bioelectron.*, 2010, **26**, 1514-1520.

S21. M. A. Ali, P. R. Solanki, M. K. Patel, H. Dhayani, V. V. Agrawal, R. John, B. D. Malhotra, *Nanoscale*, 2013, **5**, 2883-2891.

S22. G. Ma, J. Zhou, C. Tian, D. Jiang, D. Fang, H. Chen, *Anal. Chem.*, 2013, **85**, 3912-3917.

S23. R. Ahmad, N. Tripathy, Y.-B. Hahn, *Biosens. Bioelectron.*, 2013, **45**, 281-286.